EUROPEAN ORGANIZATION FOR NUCLEAR RESEARCH

CERN-PPE/97-127
19 September 1997

# Measurement of the Average Lifetime of b-Hadrons in Z Decays

The L3 Collaboration

## Abstract

We present a measurement of the average b-hadron lifetime $\tau_{\mathrm{b}}$ at the $\mathrm{e^+e^-}$ collider LEP. Using hadronic Z decays collected in the period from 1991 to 1994, two independent analyses have been performed. In the first one, the b-decay position is reconstructed as a secondary vertex of hadronic b-decay particles. The second analysis is an updated measurement of $\tau_{\mathrm{b}}$ using the impact parameter of leptons with high momentum and high transverse momentum. The combined result is

$$\tau_{\mathrm{b}} = [1549 \pm 9\,(\mathrm{stat}) \pm 15\,(\mathrm{syst})]\ \mathrm{fs}\,.$$

In addition, we measure the average charged b-decay multiplicity $\langle n_{\mathrm{b}} \rangle$ and the normalized average b-energy $\langle x_E \rangle_{\mathrm{b}}$ at LEP to be

$$\langle \mathrm{n_b} \rangle = 4.90 \pm 0.04\,(\mathrm{stat}) \pm 0.11\,(\mathrm{syst}),$$

$$\langle \mathrm{x_E} \rangle_{\mathrm{b}} = 0.709 \pm 0.004\,(\mathrm{stat} + \mathrm{syst}).$$

Submitted to *Phys. Lett. B*

# Introduction

Lifetimes of b-hadrons are basic ingredients for the determination of the Cabibbo-Kobayashi-Maskawa matrix (CKM) element $|V_{cb}|$. The measurement of the b-hadron lifetime in 1983 at SLAC [1] provided the first evidence for the hierarchy of the CKM matrix elements. Today precision measurements of the b-lifetime are made at LEP, SLC and at the Tevatron [2, 3].

All b-flavoured hadrons are expected to have a similar lifetime due to the high value of the b-quark mass. An inclusive analysis at the Z resonance results in an average of the individual lifetimes of $B^+$, $B^0_d$, $B^0_s$ and $\Lambda_b$ hadrons and their antiparticles, weighted with their production cross section. In this letter we present a measurement of $\tau_b$ using two complementary and largely uncorrelated techniques.

In the first analysis, called the secondary vertex method, the hadronic decay topology of $b\bar{b}$ events is reconstructed. The track measurements are used to determine the primary $e^+e^-$ interaction point and the decay positions of b-hadrons. The b-lifetime can be derived from the impact parameters of the b-decay products or from the distance of secondary vertices with respect to the primary event vertex.

The second analysis, the lepton impact parameter method, improves the statistical and systematic accuracy compared to our previous measurement [2]. It uses the same technique and is based on the impact parameter distribution of leptons with high momentum $p$ and high transverse momentum $p_\perp$ with respect to the nearest jet.

# Hadronic Event Selection

The L3 detector and its modeling have been described elsewhere [4–6]. The selection of hadronic events is identical to the one used for the measurement of the total hadronic cross section [7]. For the lifetime analyses only events with more than four tracks measured in the Time Expansion Chamber (TEC) are kept to ensure a good vertex reconstruction. The lepton impact parameter method has been applied to a sample of 2.9 million hadronic events collected on and near the Z resonance in the years 1991 to 1994. The secondary vertex analysis has been performed on the data sample of the year 1994 consisting of 1.5 million hadronic events with a center-of-mass energy of 91.2 GeV.

In the L3 coordinate system the direction of the $e^-$ beam defines the $z$ direction. The $xy$, or $r\phi$ plane, is the bending plane of the magnetic field, with the $x$ direction pointing to the center of the LEP ring. The coordinates $\phi$ and $\theta$ denote the azimuthal and polar angles of tracks or jets.

# A) Secondary Vertex Method

The pair production of b-quarks is characterized by two decay positions (secondary vertices) separated on average by $\approx 3$ mm from the $e^+e^-$ interaction point (primary vertex). The daughter particles of b-hadrons arise at the secondary vertices and additional particles produced in the fragmentation process originate at the primary vertex. Therefore, in contrast to Z decays into other quark species, $b\bar{b}$ events consist of three distinct vertices: one primary and two secondary. The decay points of the b-hadron and of a secondary c hadron decay can not be separated and are merged into one decay position.

## Reconstruction of Z decays into $b\bar{b}$

Hadronic jets are reconstructed from energy clusters in the calorimeter using the JADE algorithm [8] with a cut on the scaled invariant mass squared $y_{\rm cut}$ of 0.04. This results mostly in two-jet events with a jet axis resolution of 40 mrad.

The tracks in the event are associated to the closest jet. The two most energetic jets in the event have been considered to contain the original b-quarks. Both of these jets must point into a fiducial region delimited by the barrel part of the detector, $|\cos\theta| < 0.74$.

The three-vertex hypothesis is tested with tracks that fulfill the following quality cuts:

- The track should contain a minimum of 25 TEC hits and at least one hit in the Silicon Microvertex Detector (SMD) from the inner $r\phi$ ring to ensure a good extrapolation to the interaction point.
- The transverse momentum with respect to the beam axis should be greater than 300 MeV in order to restrict the uncertainty due to multiple scattering.
- Tracks from identified decays of $K^0$ and $\Lambda$ hadrons are rejected to reduce the number of downstream secondary vertices.

Tracks which satisfy the above criteria are used for the calculation of the $xy$ position of the track vertices. If the track is also well measured in the $z$ projection it has been used in the calculation of the 3D vertex position.

In order to assign tracks to one of the three vertices we consider all associations and select the most likely combination by a $\chi^2$ fit, which included lifetime and kinematical information:

$$\chi^2_{vertex} = \sum_{i=1}^{n}\left[\left(\frac{\delta_i^{r\phi}(\vec{x}_j)}{\sigma_{\delta_i^{r\phi}}}\right)^2 + \left(\frac{\delta_i^{z}(\vec{x}_j)}{\sigma_{\delta_i^{z}}}\right)^2\right] + \sum_{k=1}^{3}\left(\frac{(\vec{x}_1 - \vec{x}_{BS})\vec{e}_k}{\sigma^k_{BS}}\right)^2 - 2\sum_{i=1}^{n}\ln P_l(\eta_i)$$

$$i = 1,\cdots,\text{n tracks}, \quad j = 1,2,3 \text{ vertices}$$
$$k = x,y,z \text{ projections}, \quad l = 1,2 \text{ b hadron/fragmentation}.$$

The first two terms contain the sum of quadratic deviations of all track positions to the respective vertices in $r\phi$ and $z$. The parameter $\delta_i^{r\phi}$ denotes the impact parameter of the track in the bending plane and $\delta_i^z$ is the $z$ difference, both with respect to the vertices $\vec{x}_j$.

The associated errors $\sigma_{\delta_i}$ are defined as the sum of uncertainties from the track fit and multiple scattering, added in quadrature. The impact parameter resolution for high-energy tracks is measured to 32 $\mu$m through the distribution of the distance at which tracks of dilepton events miss each other at the interaction point. The additional multiple scattering error for tracks with an inner SMD hit is $110/(p_\perp/\,\text{GeV}\sqrt{\sin\theta})$ $\mu$m. If a track does not belong to the $z$ selected sample, the error $\sigma_{\delta_i^z}$ is set to infinity.

The primary vertex $\vec{x}_1$ is constrained to be identical to the beam spot position $\vec{x}_{BS}$, within the horizontal beam spot size of $\sigma^x_{BS} = 135$ $\mu$m, the vertical size of $\sigma^y_{BS} = 25$ $\mu$m and the longitudinal size of $\sigma^z_{BS} = 1$ cm. The average beam interaction point $\vec{x}_{BS}$ is reconstructed using tracks collected from 200 hadronic events accumulated every few minutes.

The last term in the expression for $\chi^2$ exploits the high mass and high-energy of b-quarks to distinguish b-decay from fragmentation tracks. A suitable variable for b-decay tracks is the rapidity $\eta = 1/2\ \ln(E + p_{||})/(E - p_{||})$, where $E$ stands for the energy of particles (assuming

pions) and $p_{||}$ for the momentum parallel to the jet axis [9]. $P_l(\eta_i)$ is the probability density for the rapidity of either b-decay or fragmentation tracks.

In the fit at least one track from each jet is required to originate at the primary vertex and at least three tracks at the secondary vertex to reduce fake vertices of random track crossing. Therefore the minimum number of selected tracks per jet is four. Due to the higher multiplicity of $\mathrm{b\bar{b}}$ events, the b quark content is slightly increased from 22 % to 27 %. In light-flavour events the algorithm produces artificial secondary vertices with small decay lengths compatible with zero. No attempt is made to remove this background and to enrich the fraction of b events in the hadronic sample.

The result of the $\chi^2$ fit are the three-dimensional positions $\vec{x}_j$ of the three vertices $j = 1, 2, 3$. The b flight direction is fixed to the jet axis, which resolves it better than the line connecting primary and secondary vertices. The assumption of a fixed direction allows a three-dimensional interpretation of $\chi^2$ even if no track belongs to the $z$ selected sample. An event selected in 1994 data with a high probability to be a $\mathrm{b\bar{b}}$ event is shown in figure 1.

## Lifetime Fit

Lifetime measurements with hadronic b events at LEP already reach a statistical precision that is small compared to the systematic uncertainties in modeling heavy quark decays [2,3]. Our main purpose is thus to perform a fit where the values of poorly known model parameters are determined from the data itself. The most relevant parameters are the average b-hadron energy, the average b-decay multiplicity and the background of long-lived mesons.

Two variables are sensitive to the b-lifetime. One is the impact parameter, here defined as the impact parameter of those tracks attached to the secondary vertices in the minimum $\chi^2$ configuration. The other is the decay length, which measures the distance between primary and secondary vertex. The advantage of the impact parameter is that for relativistic b-hadrons its mean value is proportional to $c\tau$, whereas the decay length is proportional to $(E/m)c\tau$. The average impact parameter of tracks from b-decays at LEP is therefore less sensitive to the b-hadron momentum and to a precise knowledge of the b-quark fragmentation parameters. We have performed two lifetime fits, one to the impact parameter distribution and the other to the decay length distribution. The comparison of both results is used to measure the value of the average b-hadron energy $E$.

The $\tau_{\mathrm{b}}$ value is obtained from a binned $\chi^2$ fit to the respective distributions, with the lifetime dependent expected distribution predicted by a Monte Carlo simulation [10]. The lifetime dependence is introduced by reweighting the simulated events according to

$$\left(\frac{\tau_{MC}}{\tau_{\mathrm{b}}}\right)^2 \frac{e^{-t_1/\tau_{\mathrm{b}}}}{e^{-t_1/\tau_{MC}}} \frac{e^{-t_2/\tau_{\mathrm{b}}}}{e^{-t_2/\tau_{MC}}} ,$$

where $t_1$ and $t_2$ are the proper times of the weakly decaying b-hadrons in jet 1 and 2 and $\tau_{MC}$ is the lifetime value in the Monte Carlo, 1.55 ps. The one-parameter lifetime fit is based on the assumption that all b-hadrons have the same lifetime.

In order to account for small discrepancies in the resolution function between data and Monte Carlo additional resolution parameters are introduced. The Monte Carlo distribution is convoluted with two Gaussian functions with a standard deviation $\sigma_{1,2}$ applied to a small fraction $f_{1,2}$ of Monte Carlo events. The resolution correction parameters have been measured by the shape of the respective distributions on the negative side.

Another important source of uncertainty concerns the background of fragmentation tracks being attached to the secondary vertices. Monte Carlo studies show that this background fraction depends on the average b-decay charged multiplicity $\langle n_{\rm b}\rangle$[1)].

Secondary vertices far from the primary event vertex tend to include one or two tracks from decays of long-lived strange hadrons, mainly $\rm K^0_s$ and $\Lambda$ decays. In the following $\langle n_{\rm K}\rangle$ denotes the fraction of $\rm K^0_s$ and $\Lambda$ hadrons produced in Z decays.

In order to make the measurement of the b-lifetime independent of the described parameters, the resolution correction parameters $f_{1,2}, \sigma_{1,2}$ , the average b-decay multiplicity $\langle n_{\rm b}\rangle$ and the fraction of long-lived hadrons $\langle n_{\rm K}\rangle$ are fitted together with $\tau_{\rm b}$. We perform a binned $\chi^2$ fit simultaneously to the multiplicity distribution and to either the impact parameter or decay length distribution.

The total number of secondary vertices used in the decay length fit is 583,972. The fit to the impact parameter distribution is performed with a total of 2,007,415 tracks. The fit results are:

$$\begin{aligned} \tau_{\rm b} &= (1564 \pm 10)\ \text{fs}\,, \\ \langle n_{\rm b}\rangle &= 4.90 \pm 0.04\,, \\ \langle n_{\rm K}\rangle &= 1.29 \pm 0.02\,, \end{aligned}$$

for the impact parameter distribution and

$$\begin{aligned} \tau_{\rm b} &= (1582 \pm 12)\ \text{fs}\,, \\ \langle n_{\rm b}\rangle &= 4.89 \pm 0.04\,, \\ \langle n_{\rm K}\rangle &= 1.33 \pm 0.05\,. \end{aligned}$$

for the decay length distribution, where the errors are statistical only.

The impact parameter and decay length distribution for the fitted parameters are shown in Fig. 2. A good agreement between data and MC is observed and the positive tail due to b-decays is clearly visible.

Fig. 3 shows the average number of tracks at the secondary vertices as a function of the decay length. The peak at zero decay length is due to tracks from light quark fragmentation. The enhancement at positive decay lengths is due to b and c events and its magnitude depends on the number of charged particles from b-decays. At very small and very big decay lengths the secondary vertex multiplicity is dominated by the constraint of a minimum of three tracks.

The $\tau_{\rm b}$ value is an average value according to the b-hadron composition in Z decays. It has been checked in a Monte Carlo study that the composition of the accepted events was consistent with the world average [11] within the statistical errors.

## Systematic Uncertainties

The contributions to the systematic error in the b-lifetime measurement and $\langle n_{\rm b}\rangle$ due to detector resolution and the incomplete knowledge of heavy-flavour hadronization and decay processes are summarized in table 1.

The agreement between data and Monte Carlo in the average number of quality tracks per event is better than 0.1 tracks, resulting in the uncertainties given in table 1. The uncertainty

[1)] Our definition includes only the direct decay products pions, charged kaons, leptons and protons, not including decay products from $\rm K^0_s$ and $\Lambda$.

in the resolution function has been estimated by varying the resolution correction parameters within errors. The uncertainty in the knowledge of the beam spot size and position is determined by varying the size of the beam spot within the accuracy of the 200-event-vertex (15 $\mu$m in x and 10 $\mu$m in y) and allowing for a bias of 10 $\mu$m in x and 5 $\mu$m in y for the central beam position. The definition of the sign of the decay length depends on the jet direction. The resolution on the jet direction is estimated from comparisons between data and Monte Carlo on a two-jet event sample. The maximum discrepancy found is 2 mrad.

The precision of the lifetime measurement is further limited due to heavy-quark physics modeling. The dominant contributions arise from the uncertainty in the inclusive description of b-decays. Theoretical uncertainties have been estimated by a variation of the model parameters as recommended by the LEP Heavy Flavour Electroweak Group in [12]. Systematic errors due to b and c fragmentation are determined by varying $\epsilon_b$ and $\epsilon_c$ in the Peterson fragmentation function [13] according to $\langle x_E \rangle_{\mathrm{b}} = 0.702 \pm 0.008$ for b fragmentation and $\langle x_E \rangle_{\mathrm{c}} = 0.484 \pm 0.008$ for c fragmentation [12]. $x_E$ is the fraction of the beam energy carried by the b or c hadron. The uncertainty in $\tau_{\mathrm{b}}$ from b fragmentation is estimated to 9 fs and 30 fs for the impact parameter and decay length measurement, respectively. The b fragmentation error has also a contribution from the uncertainty in the shape of the fragmentation function. Several models [14] have been tuned on the mean value $\langle x_E \rangle_{\mathrm{b}} = 0.702$ and the maximum shift in the lifetime found is 2 fs. The error from the uncertainty in c fragmentation has been estimated to be negligible.

An uncertainty in the shape of the b-decay multiplicity distribution is taken into account by replacing the Monte Carlo distribution with a binomial distribution of the same mean and variance as in the Monte Carlo.

Sensitivity to the modeling of c quarks, occurring as primary $\mathrm{c\bar{c}}$ events and as decay products of b-hadrons, is estimated by varying the lifetimes of c hadrons and the fraction of c hadrons in $\mathrm{c\bar{c}}$ events and b-decays. The production of the different D mesons and $\Lambda_{\mathrm{c}}$ baryons in $\mathrm{c\bar{c}}$ events is varied according to the LEP averages [12]. The branching fractions $\mathrm{B_d^0 \to D^+, {D_d}^0}$ and $\mathrm{B_s^0 \to D_s^0}$ as well as the lifetimes of c hadrons are varied following the world averages [11].

### Combination of Impact Parameter and Decay Length Results

The impact parameter and decay length measurement are within their different sensitivity to the b momentum consistent with each other. We have combined the two results and simultaneously determined $\langle x_E \rangle_{\mathrm{b}}$, taking into account the correlation between the two $\tau_{\mathrm{b}}$ measurements and assuming linear dependences on $\langle x_E \rangle_{\mathrm{b}}$ with coefficients determined from Monte Carlo, as illustrated in fig. 4. The result is

$$\begin{aligned} \tau_{\mathrm{b}} &= (1556 \pm 10 \pm 17)\ \mathrm{fs}\,, \\ \langle x_E \rangle_{\mathrm{b}} &= 0.709 \pm 0.004\,. \end{aligned}$$

The average b-decay multiplicity is

$$\langle n_{\mathrm{b}} \rangle = 4.90 \pm 0.12\,.$$

The contributions to the total systematic error of the b-lifetime are similar to those in Table 1, except the uncertainty due to the b fragmentation, which is reduced to 5 fs. The errors on $\langle x_E \rangle_{\mathrm{b}}$ and $\langle n_{\mathrm{b}} \rangle$ contain both statistical and systematic uncertainties.

# B) Lepton Impact Parameter Method

## Event Selection

Electron candidates have been identified as electromagnetic showers in the BGO calorimeter associated to a track in the TEC. The fiducial volume covered the barrel part, $|\cos\theta| < 0.69$. Hadronic background has been rejected by requiring an energetic and angular matching between TEC track and BGO cluster.

Muon candidates are identified as charged tracks in the muon spectrometer, satisfying $|\cos\theta| < 0.72$. Only muons with an associated TEC track and momentum and polar angle measurements are accepted for the analysis. Punch-through tracks from long-lived hadrons are rejected by requiring a good consistency between the track extrapolation to the center of the beam collision point.

The track quality cuts for leptons are chosen to be more stringent than in the hadron track selection because a single lepton track is sufficient to perform a lifetime fit, whereas several tracks are needed for the reconstruction of a secondary vertex. In the 1994 sample, the presence of a hit in the inner $r\phi$ layer of the SMD is required, which improves the impact parameter resolution from 112 $\mu$m to 32 $\mu$m.

The fraction of $\mathrm{b\bar{b}}$ events in the sample is enhanced by selecting leptons with high momentum and transverse momentum with respect to the closest jet. The jet parameters are redefined subtracting the lepton four-momentum. For electrons the cluster energy has to be larger than 3 GeV and the transverse momentum greater than 1 GeV. For muons the cuts are 4 GeV and 1.5 GeV, respectively.

After all cuts have been applied, a sample of 17,647 electron candidates and 23,062 muon candidates is obtained. The expected sample composition is shown in Table 2 for the 1994 detector setup.

## Lifetime fit

The inclusive b-lifetime has been determined from a maximum-likelihood fit to the distribution of the impact parameter $\delta$ in the $r\phi$ plane of the lepton candidates. The impact parameter distribution for the lepton candidates has been expressed as a convolution of two functions: the true impact parameter distribution, which depends on the lifetime of b or c hadrons, and the resolution function, which describes the smearing of $\delta$ due to finite resolution. The following likelihood function

$$\mathcal{L}(\tau_\mathrm{b}) = \prod_i^{\text{tracks}} \left(f_\mathrm{b}\mathcal{P}_\mathrm{b}(\tau_\mathrm{b};\delta_i) + f_\mathrm{bc}\mathcal{P}_\mathrm{bc}(\tau_\mathrm{b};\delta_i) + f_\mathrm{c}\mathcal{P}_\mathrm{c}(\delta_i) + f_{bkg}\mathcal{B}(\delta_i)\right) \otimes \mathcal{R}(\delta_i, \phi_i, p_\perp, \sigma_{\mathrm{FIT},i})$$

is maximized. $\mathcal{P}_\mathrm{b}$, $\mathcal{P}_\mathrm{bc}$, and $\mathcal{P}_\mathrm{c}$ are the impact parameter distributions for the prompt, cascade and charm components. They included the effects of lifetimes and the occasional mis-signing of $\delta$, due to the approximation of the b-hadron direction by the jet axis. The underlying distributions $\mathcal{P}_\mathrm{b}$, $\mathcal{P}_\mathrm{bc}$, and $\mathcal{P}_\mathrm{c}$ and the one for background tracks, $\mathcal{B}$, are extracted from Monte Carlo simulated events. $\mathcal{R}$, the track-by-track impact parameter resolution function, is parametrized as a superposition of three Gaussian functions whose standard deviations depend on the track azimuthal angle $\phi_i$, the momentum $p_\perp$ transverse to the beam, and the impact parameter error

from the track fit $\sigma_{FIT,i}$:

$$\mathcal{R}(\delta_i, \phi_i, p_\perp, \sigma_{\mathrm{FIT},i}) = \sum_{j=1}^{3} \frac{f_j}{\sqrt{2\pi}\sigma_{ij}} \exp\left(-\frac{\delta_i^2}{2\sigma_{ij}^2}\right) \qquad \text{with} \quad \sum_{j=1}^{3} f_j = 1.$$

as described in our publication [2]. $\sigma_{ij}$ denotes the impact parameter resolution for the $i^{\mathrm{th}}$ track.

In order to reduce systematic uncertainties which would otherwise limit the increase in statistical accuracy compared to our previous publication additional free parameters have been introduced in the maximum-likelihood fit. The relevant changes are:

- The parameters $f_j$ have been left free. These fractions are not supposed to be similar for primary and secondary tracks, because they follow different distributions in phase space. Monte Carlo studies show that $f_1 \approx 1$, $f_2 \approx 0$ for secondaries while $f_1 \approx 0.8$, $f_2 \approx 0.2$ for the sample enriched in primary tracks.

- The background fraction, $f_{bkg}$, is also treated as a free parameter. The background contribution $\mathcal{B}$ is almost invariant under the change $\delta \leftrightarrow -\delta$, which can be disentangled from the asymmetric shape of $\mathcal{P}_\mathrm{b}$. This approach reduces the systematic error, in particular those caused by uncertainties in the parameters $\mathrm{R_b}$ and $\mathrm{Br(b \to \ell\nu X)}$, by a sizeable amount.

The fits are performed separately for the four years of data taking, to account for changes in detector setup and performance. The results for 1993 and 1994 are shown in figure 5. Due to the SMD the resolution has improved significantly in 1994.

The different sources of systematic errors can be found in Table 1. Theoretical uncertainties have been assigned following the recommendations of the LEP Heavy Flavour Electroweak Group in [12]. We observed small dependences on the Monte Carlo parameters that govern the heavy-flavour production and decay fractions. The error due to uncertainties in the shape of the underlying distributions $\mathcal{P}$, mainly caused by Monte Carlo statistics, is combined under fit method error.

The fitted lifetimes obtained for the four data taking periods and two lepton channels agree with each other:

$$\tau_\mathrm{b}(\mathrm{e}) = (1530 \pm 23 \pm 23)\,\mathrm{fs} \qquad \tau_\mathrm{b}(\mu) = (1553 \pm 22 \pm 23)\,\mathrm{fs}\ .$$

Taking into account the correlation between uncertainties in the muon and the electron channel, the combined result from the lepton impact parameter method is:

$$\tau_\mathrm{b} = (1544 \pm 16 \pm 21)\,\mathrm{fs}\ .$$

# Combined Results

The results from the secondary vertex and lepton analysis is combined as weighted average of nine measurements. The measurements with electrons and muons in the years 1991 to 1994 are added to the result from the secondary vertex analysis in 1994 taking into account the correlations between the measurements. The statistical correlation between the lepton and secondary vertex measurement is negligible. The dominant systematic errors, the uncertainty in the underlying lepton distributions and the lepton track selection criteria on the one side and

the charm hadron composition on the other side, are also independent in both measurements. The combined result for the average b-hadron lifetime at the Z resonance is

$$\tau_{\mathrm{b}} = (1549 \pm 9 \pm 15)\,\mathrm{fs}\ ,$$

where the first error is statistical and the second is systematic. The result is in good agreement with our previous measurements of $\tau_{\mathrm{b}}$ and with the world average of $1550 \pm 20$ fs [11].

The secondary vertex analysis yields in addition a measurement of the average b-decay multiplicity and the normalized average b-energy at LEP:

$$\begin{aligned} \langle n_{\mathrm{b}} \rangle &= 4.90 \pm 0.12 \\ \langle x_E \rangle_{\mathrm{b}} &= 0.709 \pm 0.004\ . \end{aligned}$$

These precise results are improvements over the other measurements [12, 15]. The uncertainty in $\langle x_E \rangle_{\mathrm{b}}$ reached by the novel method presented here is significantly lower than in previous analyses.

# Acknowledgements

We wish to express our gratitude to the CERN accelerator divisions for the excellent performance of the LEP machine. We acknowledge the effort of all engineers and technicians who have participated in the construction and maintenance of the experiment.

# References


[1] MAC Collaboration, E. Fernandez *et al.*, Phys. Rev. Lett. **51** (1983) 1022.
MARK II Collaboration, N.S. Lockyer *et al.*, Phys. Rev. Lett. **51** (1983) 1316.

[2] L3 Collaboration, O. Adriani *et al.*, Phys. Lett. **B 317** (1993) 474.

[3] ALEPH Collaboration, D. Buskulic *et al.*, Phys. Lett. **B 314** (1993) 459.
ALEPH Collaboration, D. Buskulic *et al.*, Phys. Lett. **B 369** (1996) 151.
DELPHI Collaboration, P. Abreu *et al.*, Z. Phys. **C 63** (1994) 3.
DELPHI Collaboration, P. Abreu *et al.*, Phys. Lett. **B 377** (1996) 195.
OPAL Collaboration, P.D. Acton *et al.*, Z. Phys. **C 60** (1993) 217.
OPAL Collaboration, P.D. Acton *et al.*, Z. Phys. **C 73** (1997) 397.
SLD Collaboration, K. Abe *et al.*, Phys. Rev. Lett. **75** (1997) 3624.
CDF Collaboration, F. Abe *et al.*, Phys. Rev. Lett. **71** (1993) 3421.

[4] L3 Collaboration, M. Acciarri *et al.*, Nucl. Instr. and Meth. **A 351** (1994) 300.

[5] The L3 Collaboration, B. Adeva *et al.*, Nucl. Instr. and Meth. **A 289** (1990) 35.
M. Chemarin *et al.*, Nucl. Instr. and Meth. **A 349** (1994) 345.
A. Adam *et al.*, Nucl. Instr. and Meth. **A 383** (1996) 342.
I.C. Brock *et al.*, Nucl. Instr. and Meth. **A 381** (1996) 236.

[6] The L3 detector simulation is based on GEANT Version 3.15.
R. Brun *et al.*, *GEANT 3*, CERN-DD/EE/84-1 (Revised), 1987.
The GHEISHA program (H. Fesefeldt, RWTH Aachen Report PITHA 85/02 (1985)) is used to simulate hadronic interactions.

[7] L3 Collaboration, M. Acciarri *et al.*, Z. Phys. **C62** (1994) 551.

[8] JADE Collaboration, W. Bartel *et al.*, Z. Phys. **C33** (1986) 23.

[9] DELPHI Collaboration, P. Abreu *et al.*, Z. Phys. **C68** (1995) 353.

[10] T. Sjöstrand, Comp. Phys. Comm. **39** (1986) 347;
T. Sjöstrand and M. Bengtsson, Comp. Phys. Comm. **43** (1987) 367.

[11] Particle Data Group, R. M. Barnett *et al.*, Phys. Rev. **D54** (1996).

[12] The LEP Experiments: ALEPH, DELPHI, L3, OPAL, Nucl. Instr. and Meth. **A 378** (1996) 101, and references therein.

[13] C. Peterson, D. Schlatter, I. Schmitt and P. M. Zerwas, Phys. Rev. **D27** (1983) 105.

[14] M. G. Bowler, Z. Phys. **C11** (1981) 169.
P. Collins and T. Spiller, J. Phys. **G11** (1985) 1289.
V. G. Kartvelishvili, A. K. Likhoded and V. A. Petrov, Phys. Lett. **B78** (1978) 615.

[15] ARGUS Collaboration, H. Albrecht *et al.*, X.Y. et al. Z. Phys. **C 54** (1992) 20.

OPAL Collaboration, R. Akers *et al.*, Z. Phys. **C 61** (1994) 209.

DELPHI Collaboration, P. Abreu *et al.*, Phys. Lett. **B 347** (1995) 447.

CLEO Collaboration, P. Avery *et al.*, "Charged Particle Multiplicity in B-Meson Decay", Preprint CLEO CONF 96-28.

## The L3 Collaboration:


M.Acciarri,[28] O.Adriani,[17] M.Aguilar-Benitez,[27] S.Ahlen,[11] J.Alcaraz,[27] G.Alemanni,[23] J.Allaby,[18] A.Aloisio,[30] G.Alverson,[12] M.G.Alviggi,[30] G.Ambrosi,[20] H.Anderhub,[50] V.P.Andreev,[39] T.Angelescu,[13] F.Anselmo,[9] A.Arefiev,[29] T.Azemoon,[3] T.Aziz,[10] P.Bagnaia,[38] L.Baksay,[45] R.C.Ball,[3] S.Banerjee,[10] Sw.Banerjee,[10] K.Banicz,[47] A.Barczyk,[50,48] R.Barillère,[18] L.Barone,[38] P.Bartalini,[35] A.Baschirotto,[28] M.Basile,[9] R.Battiston,[35] A.Bay,[23] F.Becattini,[17] U.Becker,[16] F.Behner,[50] J.Berdugo,[27] P.Berges,[16] B.Bertucci,[35] B.L.Betev,[50] S.Bhattacharya,[10] M.Biasini,[18] A.Biland,[50] G.M.Bilei[35] J.J.Blaising,[4] S.C.Blyth,[36] G.J.Bobbink,[2] R.Bock,[1] A.Böhm,[1] L.Boldizsar,[14] B.Borgia,[38] D.Bourilkov,[50] M.Bourquin,[20] D.Boutigny,[4] S.Braccini,[20] J.G.Branson,[41] V.Brigljevic,[50] I.C.Brock,[36] A.Buffini,[17] A.Buijs,[46] J.D.Burger,[16] W.J.Burger,[20] J.Busenitz,[45] X.D.Cai,[16] M.Campanelli,[50] M.Capell,[16] G.Cara Romeo,[9] G.Carlino,[30] A.M.Cartacci,[17] J.Casaus,[27] G.Castellini,[17] F.Cavallari,[38] N.Cavallo,[30] C.Cecchi,[20] M.Cerrada,[27] F.Cesaroni,[24] M.Chamizo,[27] Y.H.Chang,[52] U.K.Chaturvedi,[19] S.V.Chekanov,[32] M.Chemarin,[26] A.Chen,[52] G.Chen,[7] G.M.Chen,[7] H.F.Chen,[21] H.S.Chen,[7] M.Chen,[16] G.Chiefari,[30] C.Y.Chien,[5] L.Cifarelli,[40] F.Cindolo,[9] C.Civinini,[17] I.Clare,[16] R.Clare,[16] H.O.Cohn,[33] G.Coignet,[4] A.P.Colijn,[2] N.Colino,[27] S.Costantini,[8] F.Cotorobai,[13] B.de la Cruz,[27] A.Csilling,[14] T.S.Dai,[16] R.D'Alessandro,[17] R.de Asmundis,[30] A.Degré,[4] K.Deiters,[48] P.Denes,[37] F.DeNotaristefani,[38] D.DiBitonto,[45] M.Diemoz,[38] D.van Dierendonck,[2] F.Di Lodovico,[50] C.Dionisi,[38] M.Dittmar,[50] A.Dominguez,[41] A.Doria,[30] M.T.Dova,[19,♯] E.Drago,[30] D.Duchesneau,[4] P.Duinker,[2] I.Duran,[42] S.Dutta,[10] S.Easo,[35] Yu.Efremenko,[33] H.El Mamouni,[26] A.Engler,[36] F.J.Eppling,[16] F.C.Erné,[2] J.P.Ernenwein,[26] P.Extermann,[20] M.Fabre,[48] R.Faccini,[38] S.Falciano,[38] A.Favara,[17] J.Fay,[26] O.Fedin,[39] M.Felcini,[50] B.Fenyi,[45] T.Ferguson,[36] D.Fernandez,[27] F.Ferroni,[38] H.Fesefeldt,[1] E.Fiandrini,[35] J.H.Field,[20] F.Filthaut,[36] P.H.Fisher,[16] I.Fisk,[41] G.Forconi,[16] L.Fredj,[20] K.Freudenreich,[50] C.Furetta,[28] Yu.Galaktionov,[29,16] S.N.Ganguli,[10] P.Garcia-Abia,[49] S.S.Gau,[12] S.Gentile,[38] J.Gerald,[5] N.Gheordanescu,[13] S.Giagu,[38] S.Goldfarb,[23] J.Goldstein,[11] Z.F.Gong,[21] A.Gougas,[5] G.Gratta,[34] M.W.Gruenewald,[8] V.K.Gupta,[37] A.Gurtu,[10] L.J.Gutay,[47] B.Hartmann,[1] A.Hasan,[31] D.Hatzifotiadou,[9] T.Hebbeker,[8] A.Hervé,[18] W.C.van Hoek,[32] H.Hofer,[50] S.J.Hong,[44] H.Hoorani,[36] S.R.Hou,[52] G.Hu,[5] V.Innocente,[18] K.Jenkes,[1] B.N.Jin,[7] L.W.Jones,[3] P.de Jong,[18] I.Josa-Mutuberria,[27] A.Kasser,[23] R.A.Khan,[19] D.Kamrad,[49] Yu.Kamyshkov,[33] J.S.Kapustinsky,[25] Y.Karyotakis,[4] M.Kaur,[19,◇] M.N.Kienzle-Focacci,[20] D.Kim,[38] D.H.Kim,[44] J.K.Kim,[44] S.C.Kim,[44] Y.G.Kim,[44] W.W.Kinnison,[25] A.Kirkby,[34] D.Kirkby,[34] J.Kirkby,[18] D.Kiss,[14] W.Kittel,[32] A.Klimentov,[16,29] A.C.König,[32] A.Kopp,[49] I.Korolko,[29] V.Koutsenko,[16,29] R.W.Kraemer,[36] W.Krenz,[1] A.Kunin,[16,29] P.Lacentre,[49,♮,♯] P.Ladron de Guevara,[27] G.Landi,[17] C.Lapoint,[16] K.Lassila-Perini,[50] P.Laurikainen,[22] M.Lebeau,[18] A.Lebedev,[16] P.Lebrun,[26] P.Lecomte,[50] P.Lecoq,[18] P.Le Coultre,[50] H.J.Lee,[8] C.Leggett,[3] J.M.Le Goff,[18] R.Leiste,[49] E.Leonardi,[38] P.Levtchenko,[39] C.Li,[21] C.H.Lin,[52] W.T.Lin,[52] F.L.Linde,[2,18] L.Lista,[30] Z.A.Liu,[7] W.Lohmann,[49] E.Longo,[38] W.Lu,[34] Y.S.Lu,[7] K.Lübelsmeyer,[1] C.Luci,[38] D.Luckey,[16] L.Luminari,[38] W.Lustermann,[48] W.G.Ma,[21] M.Maity,[10] G.Majumder,[10] L.Malgeri,[38] A.Malinin,[29] C.Maña,[27] D.Mangeol,[32] S.Mangla,[10] P.Marchesini,[50] A.Marin,[11] J.P.Martin,[26] F.Marzano,[38] G.G.G.Massaro,[2] D.McNally,[18] S.Mele,[30] L.Merola,[30] M.Meschini,[17] W.J.Metzger,[32] M.von der Mey,[1] Y.Mi,[23] A.Mihul,[13] A.J.W.van Mil,[32] H.Milcent,[18] G.Mirabelli,[38] J.Mnich,[18] P.Molnar,[8] B.Monteleoni,[17] R.Moore,[3] S.Morganti,[38] T.Moulik,[10] R.Mount,[34] F.Muheim,[20] A.J.M.Muijs,[2] S.Nahn,[16] M.Napolitano,[30] F.Nessi-Tedaldi,[50] H.Newman,[34] T.Niessen,[1] A.Nippe,[23] A.Nisati,[38] H.Nowak,[49] Y.D.Oh,[44] H.Opitz,[1] G.Organtini,[38] R.Ostonen,[22] C.Palomares,[27] D.Pandoulas,[1] S.Paoletti,[38] P.Paolucci,[30] H.K.Park,[36] I.H.Park,[44] G.Pascale,[38] G.Passaleva,[18] S.Patricelli,[30] T.Paul,[12] M.Pauluzzi,[35] C.Paus,[18] F.Pauss,[50] D.Peach,[18] Y.J.Pei,[1] S.Pensotti,[28] D.Perret-Gallix,[4] B.Petersen,[32] S.Petrak,[8] A.Pevsner,[5] D.Piccolo,[30] M.Pieri,[17] P.A.Piroué,[37] E.Pistolesi,[28] V.Plyaskin,[29] M.Pohl,[50] V.Pojidaev,[29,17] H.Postema,[16] N.Produit,[20] D.Prokofiev,[39] G.Rahal-Callot,[50] N.Raja,[10] P.G.Rancoita,[28] M.Rattaggi,[28] G.Raven,[41] P.Razis,[31] K.Read,[33] D.Ren,[50] M.Rescigno,[38] S.Reucroft,[12] T.van Rhee,[46] S.Riemann,[49] K.Riles,[3] O.Rind,[3] A.Robohm,[50] J.Rodin,[16] B.P.Roe,[3] L.Romero,[27] S.Rosier-Lees,[4] Ph.Rosselet,[23] W.van Rossum,[46] S.Roth,[1] J.A.Rubio,[18] D.Ruschmeier,[8] H.Rykaczewski,[50] J.Salicio,[18] E.Sanchez,[27] M.P.Sanders,[32] M.E.Sarakinos,[22] S.Sarkar,[10] G.Sauvage,[4] C.Schäfer,[1] V.Schegelsky,[39] S.Schmidt-Kaerst,[1] D.Schmitz,[1] M.Schneegans,[4] N.Scholz,[50] H.Schopper,[51] D.J.Schotanus,[32] J.Schwenke,[1] G.Schwering,[1] C.Sciacca,[30] D.Sciarrino,[20] L.Servoli,[35] S.Shevchenko,[34] N.Shivarov,[43] V.Shoutko,[29] J.Shukla,[25] E.Shumilov,[29] A.Shvorob,[34] T.Siedenburg,[1] D.Son,[44] V.Soulimov,[30] B.Smith,[16] P.Spillantini,[17] M.Steuer,[16] D.P.Stickland,[37] H.Stone,[37] B.Stoyanov,[43] A.Straessner,[1] K.Strauch,[15] K.Sudhakar,[10] G.Sultanov,[19] L.Z.Sun,[21] G.F.Susinno,[20] H.Suter,[50] J.D.Swain,[19] X.W.Tang,[7] L.Tauscher,[6] L.Taylor,[12] Samuel C.C.Ting,[16] S.M.Ting,[16] S.C.Tonwar,[10] J.Tóth,[14] C.Tully,[37] H.Tuchscherer,[45] K.L.Tung,[7] Y.Uchida,[16] J.Ulbricht,[50] U.Uwer,[18] E.Valente,[38] R.T.Van de Walle,[32] G.Vesztergombi,[14] I.Vetlitsky,[29] G.Viertel,[50] M.Vivargent,[4] R.Völkert,[49] H.Vogel,[36] H.Vogt,[49] I.Vorobiev,[18,29] A.A.Vorobyov,[39] A.Vorvolakos,[31] M.Wadhwa,[6] W.Wallraff,[1] J.C.Wang,[16] X.L.Wang,[21] Z.M.Wang,[21] A.Weber,[1] S.X.Wu,[19] S.Wynhoff,[1] J.Xu,[11] Z.Z.Xu,[21] B.Z.Yang,[21] C.G.Yang,[7] X.Y.Yao,[7] J.B.Ye,[21] S.C.Yeh,[52] J.M.You,[36] An.Zalite,[39] Yu.Zalite,[39] P.Zemp,[50] Y.Zeng,[1] Z.Zhang,[7] Z.P.Zhang,[21] B.Zhou,[11] Y.Zhou,[3] G.Y.Zhu,[7] R.Y.Zhu,[34] A.Zichichi,[9,18,19] F.Ziegler.[49]

1 I. Physikalisches Institut, RWTH, D-52056 Aachen, FRG[§]
III. Physikalisches Institut, RWTH, D-52056 Aachen, FRG[§]
2 National Institute for High Energy Physics, NIKHEF, and University of Amsterdam, NL-1009 DB Amsterdam, The Netherlands
3 University of Michigan, Ann Arbor, MI 48109, USA
4 Laboratoire d'Annecy-le-Vieux de Physique des Particules, LAPP,IN2P3-CNRS, BP 110, F-74941 Annecy-le-Vieux CEDEX, France
5 Johns Hopkins University, Baltimore, MD 21218, USA
6 Institute of Physics, University of Basel, CH-4056 Basel, Switzerland
7 Institute of High Energy Physics, IHEP, 100039 Beijing, China[△]
8 Humboldt University, D-10099 Berlin, FRG[§]
9 University of Bologna and INFN-Sezione di Bologna, I-40126 Bologna, Italy
10 Tata Institute of Fundamental Research, Bombay 400 005, India
11 Boston University, Boston, MA 02215, USA
12 Northeastern University, Boston, MA 02115, USA
13 Institute of Atomic Physics and University of Bucharest, R-76900 Bucharest, Romania
14 Central Research Institute for Physics of the Hungarian Academy of Sciences, H-1525 Budapest 114, Hungary[‡]
15 Harvard University, Cambridge, MA 02139, USA
16 Massachusetts Institute of Technology, Cambridge, MA 02139, USA
17 INFN Sezione di Firenze and University of Florence, I-50125 Florence, Italy
18 European Laboratory for Particle Physics, CERN, CH-1211 Geneva 23, Switzerland
19 World Laboratory, FBLJA Project, CH-1211 Geneva 23, Switzerland
20 University of Geneva, CH-1211 Geneva 4, Switzerland
21 Chinese University of Science and Technology, USTC, Hefei, Anhui 230 029, China[△]
22 SEFT, Research Institute for High Energy Physics, P.O. Box 9, SF-00014 Helsinki, Finland
23 University of Lausanne, CH-1015 Lausanne, Switzerland
24 INFN-Sezione di Lecce and Universitá Degli Studi di Lecce, I-73100 Lecce, Italy
25 Los Alamos National Laboratory, Los Alamos, NM 87544, USA
26 Institut de Physique Nucléaire de Lyon, IN2P3-CNRS,Université Claude Bernard, F-69622 Villeurbanne, France
27 Centro de Investigaciones Energeticas, Medioambientales y Tecnologicas, CIEMAT, E-28040 Madrid, Spain[♭]
28 INFN-Sezione di Milano, I-20133 Milan, Italy
29 Institute of Theoretical and Experimental Physics, ITEP, Moscow, Russia
30 INFN-Sezione di Napoli and University of Naples, I-80125 Naples, Italy
31 Department of Natural Sciences, University of Cyprus, Nicosia, Cyprus
32 University of Nijmegen and NIKHEF, NL-6525 ED Nijmegen, The Netherlands
33 Oak Ridge National Laboratory, Oak Ridge, TN 37831, USA
34 California Institute of Technology, Pasadena, CA 91125, USA
35 INFN-Sezione di Perugia and Universitá Degli Studi di Perugia, I-06100 Perugia, Italy
36 Carnegie Mellon University, Pittsburgh, PA 15213, USA
37 Princeton University, Princeton, NJ 08544, USA
38 INFN-Sezione di Roma and University of Rome, "La Sapienza", I-00185 Rome, Italy
39 Nuclear Physics Institute, St. Petersburg, Russia
40 University and INFN, Salerno, I-84100 Salerno, Italy
41 University of California, San Diego, CA 92093, USA
42 Dept. de Fisica de Particulas Elementales, Univ. de Santiago, E-15706 Santiago de Compostela, Spain
43 Bulgarian Academy of Sciences, Central Lab. of Mechatronics and Instrumentation, BU-1113 Sofia, Bulgaria
44 Center for High Energy Physics, Korea Adv. Inst. of Sciences and Technology, 305-701 Taejon, Republic of Korea
45 University of Alabama, Tuscaloosa, AL 35486, USA
46 Utrecht University and NIKHEF, NL-3584 CB Utrecht, The Netherlands
47 Purdue University, West Lafayette, IN 47907, USA
48 Paul Scherrer Institut, PSI, CH-5232 Villigen, Switzerland
49 DESY-Institut für Hochenergiephysik, D-15738 Zeuthen, FRG
50 Eidgenössische Technische Hochschule, ETH Zürich, CH-8093 Zürich, Switzerland
51 University of Hamburg, D-22761 Hamburg, FRG
52 High Energy Physics Group, Taiwan, China

§ Supported by the German Bundesministerium für Bildung, Wissenschaft, Forschung und Technologie
‡ Supported by the Hungarian OTKA fund under contract numbers T14459 and T24011.
♭ Supported also by the Comisión Interministerial de Ciencia y Tecnología
♯ Also supported by CONICET and Universidad Nacional de La Plata, CC 67, 1900 La Plata, Argentina
♮ Supported by Deutscher Akademischer Austauschdienst.
♢ Also supported by Panjab University, Chandigarh-160014, India
△ Supported by the National Natural Science Foundation of China.

| | a) Secondary Vertex Method | | | b) Lepton Method | |
|---|---|---|---|---|---|
| Error source | $\Delta\tau_b^{IP}$ (fs) | $\Delta\tau_b^{DL}$ (fs) | $\Delta n_{\rm b}$ | $\Delta\tau_{\rm b}^{e}(fs)$ | $\Delta\tau_{\rm b}^{\mu}(fs)$ |
| Reconstructed track multiplicity | 5 | 2 | 0.04 | - | - |
| Resolution function | 5 | 5 | 0.07 | 3 | 2 |
| TEC calibration and SMD alignment | 3 | 3 | <0.01 | 15 | 10 |
| Beam spot size and position | 6 | 7 | <0.01 | 6 | 6 |
| Jet direction resolution | 5 | 5 | <0.01 | 4 | 5 |
| Lepton Selection | - | - | - | 15 | 15 |
| **Sum of Detector Uncertainties** | 11 | 11 | 0.08 | 22 | 19 |
| b fragmentation | 9 | 30 | 0.02 | 5 | 3 |
| c fragmentation | <1 | 2 | <0.01 | 1 | 1 |
| b-decay multiplicity distribution | 4 | 4 | 0.06 | - | - |
| D fraction in $c\bar{c}$ events | 3 | 2 | <0.01 | <1 | <1 |
| D content in b-decays | 11 | 10 | 0.04 | 4 | 4 |
| D lifetimes | 3 | 2 | <0.01 | <1 | <1 |
| $R_b$ | 4 | 4 | 0.02 | <1 | <1 |
| $R_c$ | 1 | 1 | 0.01 | 1 | 1 |
| Semileptonic branching fractions | - | - | - | 1 | 1 |
| Inclusive lepton spectra | - | - | - | 3 | 5 |
| Fit Method | 2 | 2 | <0.01 | 16 | 14 |
| **Heavy Quark Physics Modeling** | 16 | 32 | 0.08 | 18 | 16 |

Table 1: Systematic errors in the measurement of $\tau_{\rm b}$ with a) secondary vertices and b) with leptons. $\Delta\tau_b^{IP}$ is the error for the impact parameter and $\Delta\tau_b^{DL}$ for the decay length method. The corresponding errors in the b-decay multiplicity $\Delta n_{\rm b}$ are also given. $\Delta\tau_{\rm b}^{e}$ and $\Delta\tau_{\rm b}^{\mu}$ show the errors from the lepton measurement for electrons and muons, respectively.

| Composition (1994) | Electrons | Muons |
|---|---|---|
| $b \to lX$ (Prompt) | 83.1% | 76.2% |
| $b \to c \to lX$ (Cascade) | 9.6% | 9.1% |
| $c \to lX$ (Charm) | 4.6% | 7.8% |
| Background | 2.7% | 6.9% |

Table 2: Composition of the 1994 sample of selected lepton candidates, as estimated from the Monte Carlo simulation.

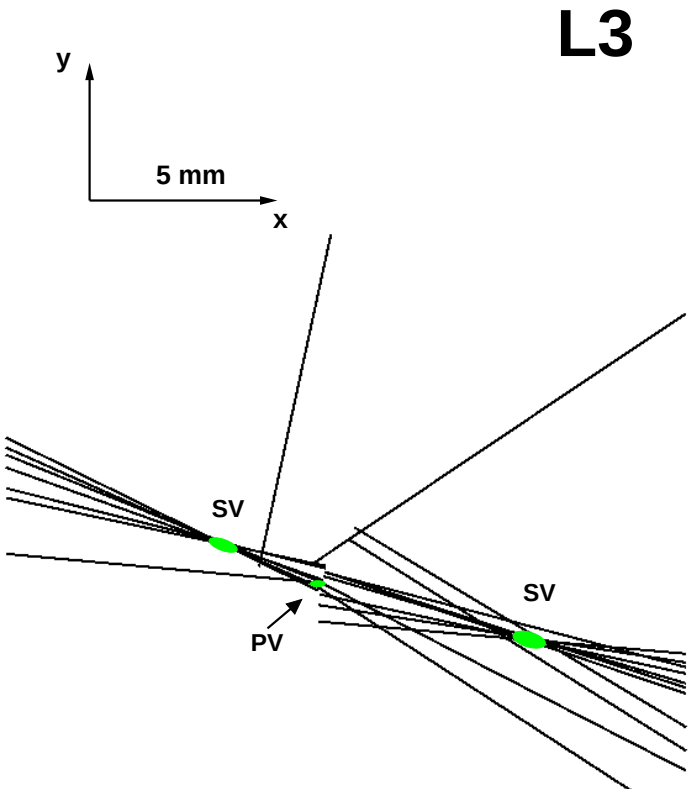


Figure 1: A $b\bar{b}$ candidate event in 1994 data shown in the $r\phi$ plane of the L3 detector. The secondary vertices (SV) in both jets of the event are separated from the primary vertex (PV) by more than five standard deviations. The shaded ellipses represent the positions of the calculated vertices within one standard deviation.

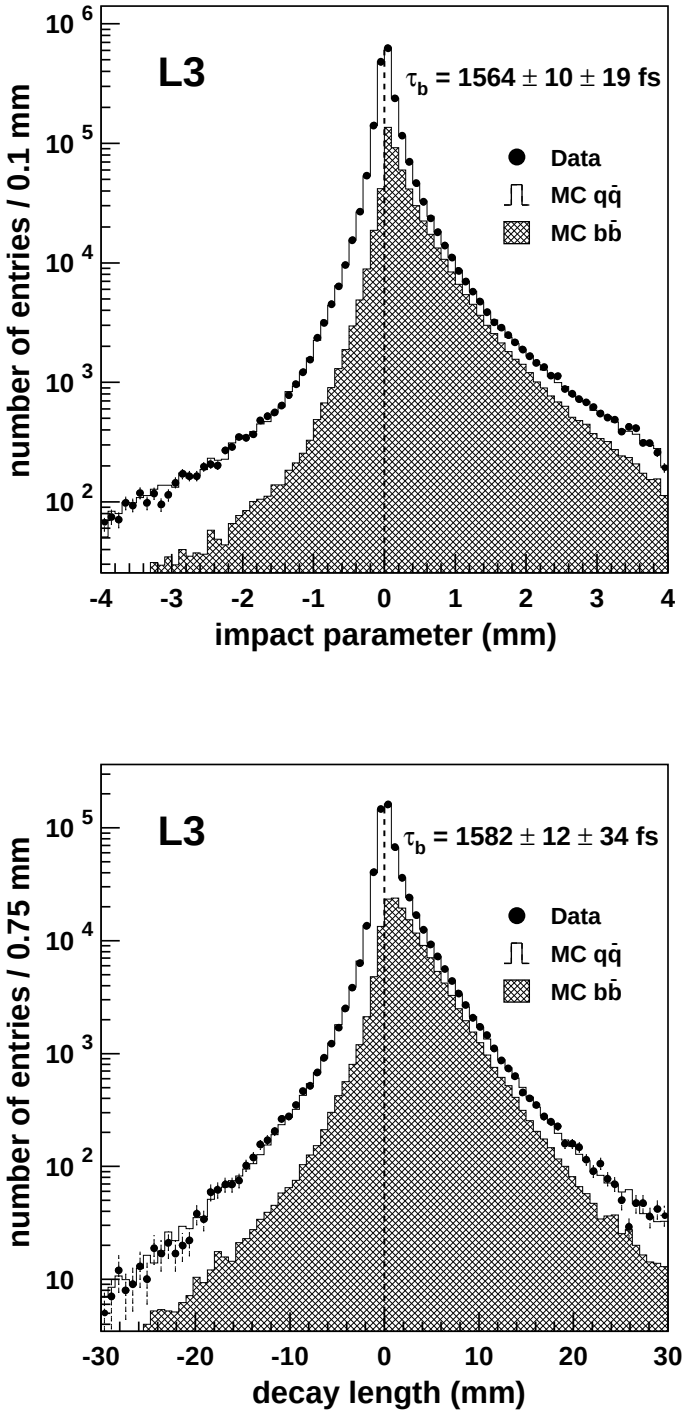


Figure 2: a) Impact parameter distribution of tracks from secondary vertices. The points represent the 1994 data and the histogram shows the MC distribution for the fitted lifetime $\tau_b = 1564$ fs. The b component in the MC sample is indicated by the shaded histogram. b) Decay length distribution of reconstructed secondary vertices. The points represent the 1994 data and the histogram shows the MC distribution for the fit result $\tau_b = 1582$ fs. The b component in the MC sample is indicated by the shaded histogram.

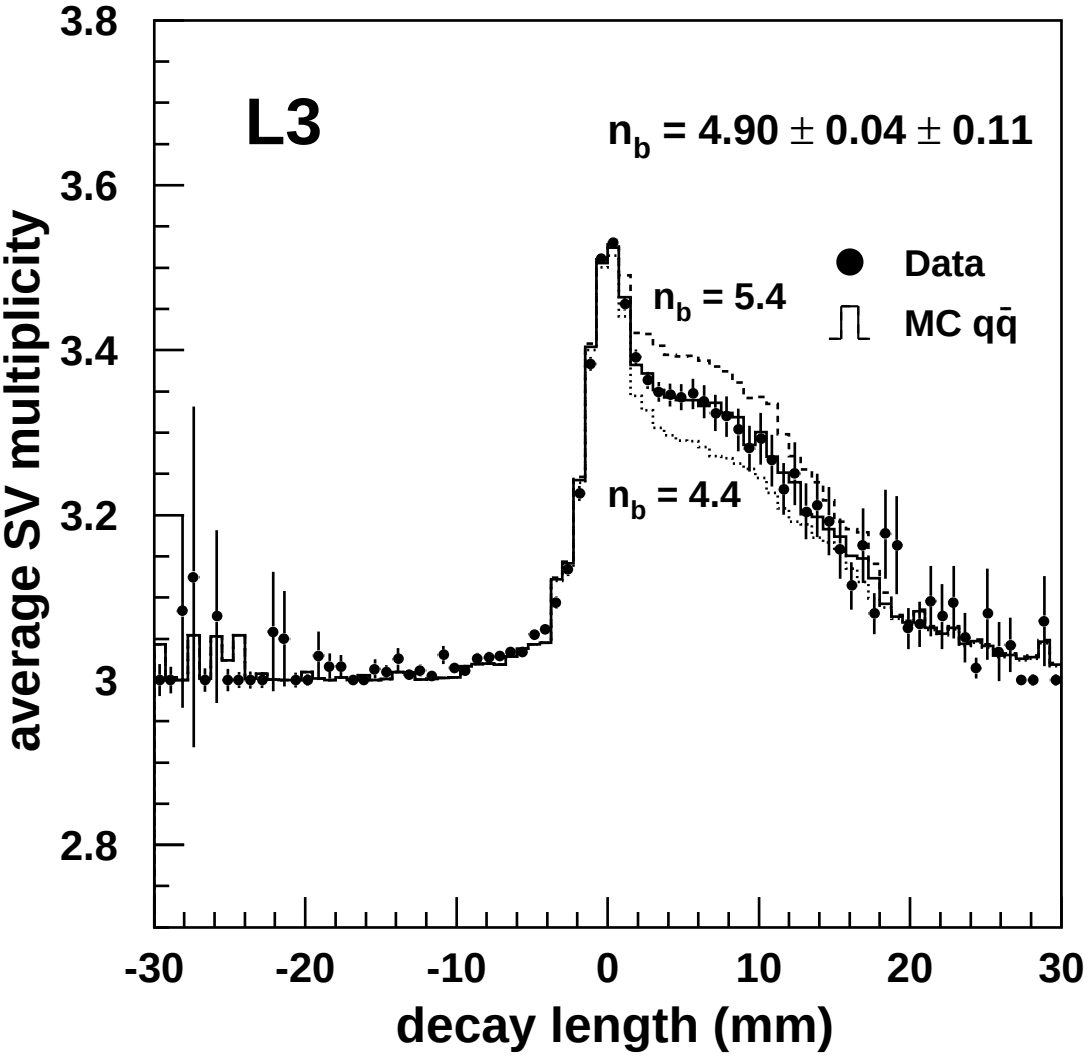


Figure 3: Average multiplicity of tracks at the secondary vertices as a function of the decay length. The points represent the 1994 data and the histogram shows the MC distribution for the fitted average b-decay multiplicity $\langle n_{\rm b} \rangle$ =4.9. The dotted (dashed) line indicates the multiplicity distribution for $\langle n_{\rm b} \rangle$ =4.4(5.4).

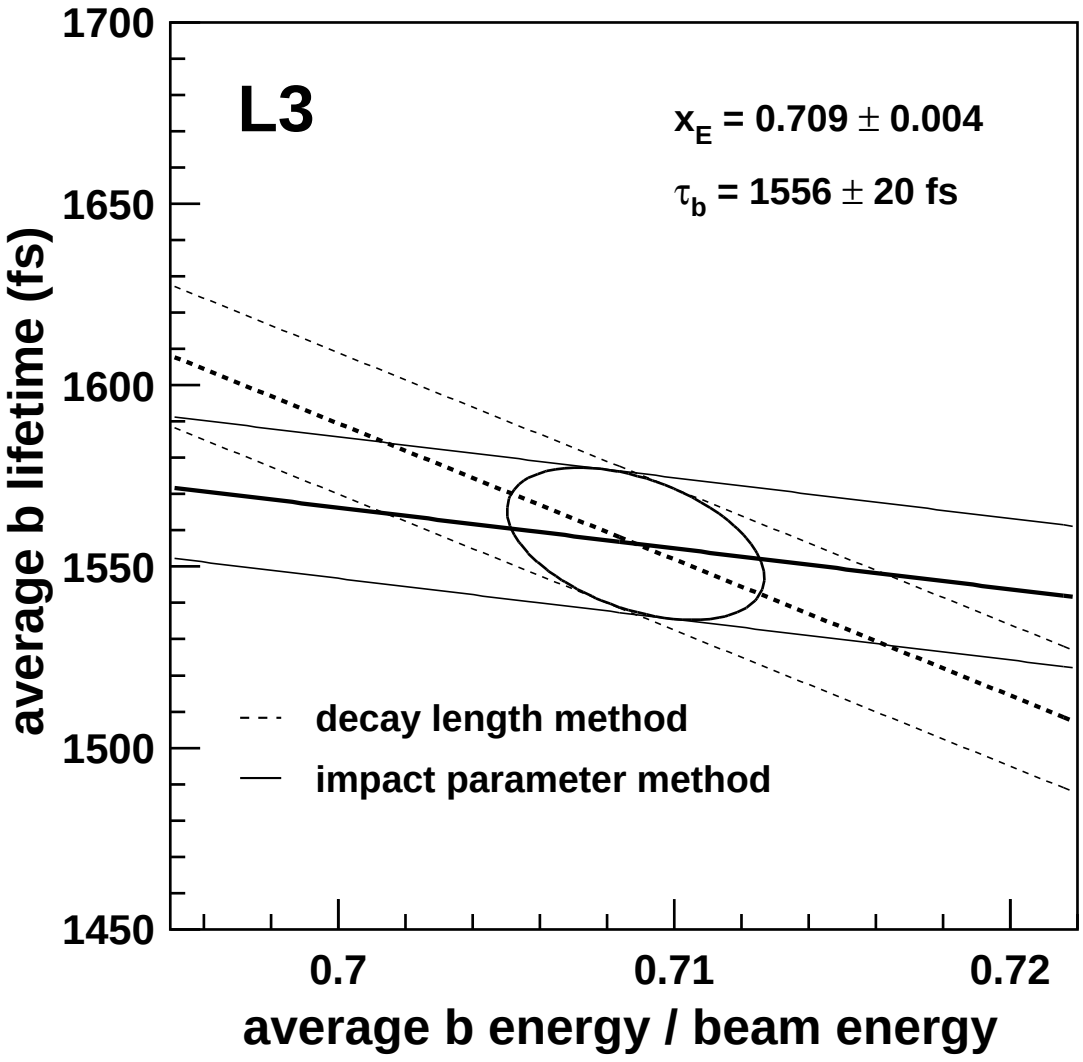


Figure 4: Dependence on $\langle x_E \rangle_\mathrm{b}$ of the hadronic impact parameter (full line) and the decay length (dashed line) measurement. The central values are shown together with the upper and lower one sigma bounds. Both measurements are compatible with each other at an average b-energy of $\langle x_E \rangle_\mathrm{b} = 0.709 \pm 0.004$ and a b-lifetime of $\tau_\mathrm{b} = 1556 \pm 20$ fs.

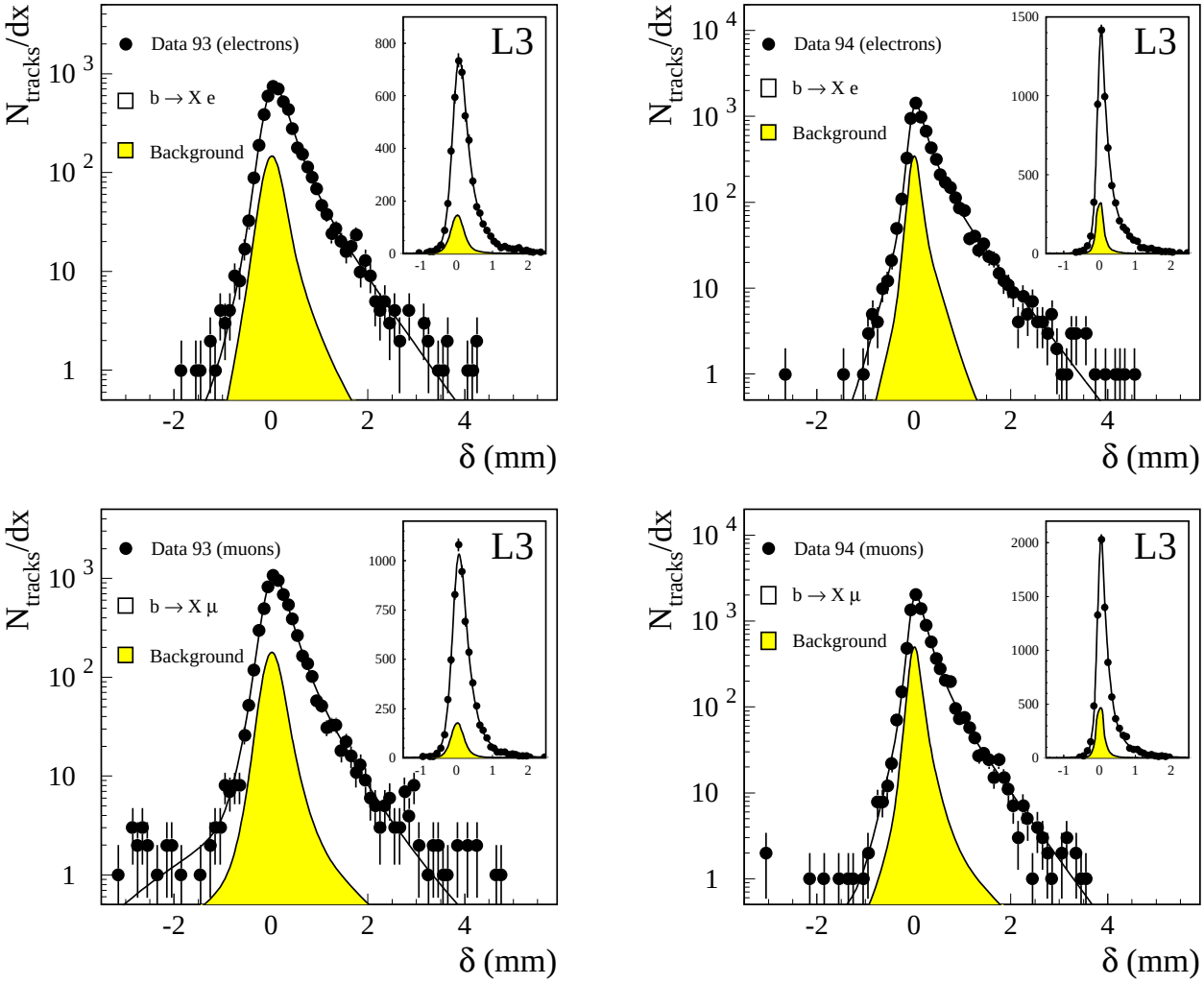


Figure 5: Results of the maximum-likelihood fits for the lepton impact parameter distribution in 1993 and 1994. Both logarithmic and linear scales are shown.